

## Chapter 2

### A Low-Velocity Intense Source of Atoms from a Magneto-Optical Trap

#### 2.1 Introduction

Cold atomic beams are useful in a variety of applications: in ultra-high resolution spectroscopy, as frequency standards, and in studies of cold atomic collisions [46]. An intense beam of cold atoms is valuable for atom interferometers [47], particularly those sensing rotational and gravitational effects. A cold atomic beam coupled into an atom fiber guide [48] will provide much larger guided atom flux. Current experiments studying Bose-Einstein condensation [1] and trapping of radioactive atoms for fundamental symmetry tests [49, 30] require a system of two magneto-optical traps (MOTs) with the capturing and the measurement processes separated in space. Our experiment reveals a simple and efficient way to transfer atoms between two MOT's via a cold atomic beam.

Many examples of cold atomic beams have been demonstrated, such as Zeeman slowers [50, 7], chirped-cooled beams [8], and beams slowed by broadband light [51] or isotropic light [52]. These beams all experience serious transverse diffusion effects as the atoms are slowed to very low velocities ( $\lesssim 15$  m/s). This causes a loss of atoms and reduced collimation. To counteract these effects, slow atoms are passed through a two-dimensional MOT, or atom funnel, to compress and cool them [20, 22, 23]. To date, the brightest slow beams employ this technique and include a beam of Na atoms traveling 2.7 m/s with a brightness of  $3 \times 10^{11}$  atoms/sr/s [20], and a beam of Ne\* traveling 19 m/s with a brightness of  $3 \times 10^{10}$  atoms/sr/s [22]. In contrast, we have created a low-velocity intense source (LVIS) of atoms with a brightness of  $5 \times 10^{12}$  atoms/sr/s. This atomic beam, the brightest beam of atoms moving slow enough to be easily captured by a MOT ( $\lesssim 20$  m/s), offers the advantage of simplicity, for it is made merely by adding a small modification to the simple vapor cell magneto-optical trap (VCMOT) [15].

In this Chapter we report a detailed study of the LVIS beam. We observed the longitudinal velocity distribution by making time-of-flight studies; and we obtained transverse velocity distributions and absolute measures of both pulsed and continuous brightness by adding atomic beam fluorescence measurements. Our model of the system explains most of our results quantitatively, and all of them qualitatively.

## 2.2 Description

The LVIS system is nearly identical to a standard VCMOT with six orthogonal intersecting laser beams. The only difference is that one of the six trapping laser beams has a narrow dark column in its center. Atoms in the low-velocity tail of the thermal vapor enter the VCMOT trapping volume and slow down. After they diffuse into the trap center, they enter the central column (“extraction column”) and are accelerated out of the trap by the counter-propagating laser beam (“forcing beam”). The velocity of the extracted atoms is determined by the number of photons they scatter from the forcing beam before leaving the trap. A key feature of this scheme is that these extracted atoms are continuously apertured by laser light along the beam. Those diverging atoms that move out of the extraction column are recaptured and returned to the trap center. This mechanism of recycling the diverging atoms provides a very efficient way of transferring trapped atoms into a collimated atomic beam.

The atomic beam flux is determined by the capture rate of the VCMOT. In a conventional VCMOT, the equilibrium number of trapped atoms  $N_{\text{eq}}$  is the steady-state solution to the differential equation

$$\dot{N} = R - N/r_c.$$

Then  $N_{\text{eq}} = R/r_c$ , where  $R$  is the capture rate and  $r_c$  is the collisional loss rate[15, 32]. In LVIS, most of the atoms are “lost” into the atomic beam. An additional term is then added to describe the LVIS beam flux  $F = N/r_t$ , where  $r_t$  is the rate of transferring atoms into the beam. The steady-state solution to

$$\dot{N} = R - N/r_c - N/r_t$$

is given by  $F=R/(1+r_c/r_t)$ . Typically  $r_c \ll r_t$ , e.g.,  $1/r_c = 1.0$  sec and  $1/r_t = 30$  msec, so  $F \approx R$ .

The collisional loss also affects atoms in the beam. Since it takes much less energy to knock an atom out of the LVIS beam than out of a VCMOT, the beam collisional loss rate is roughly 5 times that of the VCMOT. The trade-off between collection rate of the VCMOT and collisional loss rate from the LVIS beam limits the flux and determines the optimum thermal vapor pressure ( $\sim 1 \times 10^{-7}$  Torr). The low-energy collisional cross section in Ref. [53] agrees well with the dependence of collimation and flux on Rb vapor pressure that we observe with LVIS.

## 2.3 Experimental Setup

A schematic of the  $^{87}\text{Rb}$  LVIS apparatus is shown in Fig. 2.1. A Ti:Sapphire ring laser provides about 500 mW of “trapping” light at a typical frequency 30 MHz detuned from the  $5s \ ^2S_{1/2}(F=2) \rightarrow 5p \ ^2P_{3/2}(F'=3)$  transition. A diode laser supplies 20 mW of “repump” light, tuned to the  $5s \ ^2S_{1/2}(F=1) \rightarrow 5p \ ^2P_{3/2}(F'=2)$  transition. As in a conventional VCMOT, the trapping beam is split into three beams which intersect inside a vacuum chamber containing Rb vapor. Each of the three beams is reflected back in

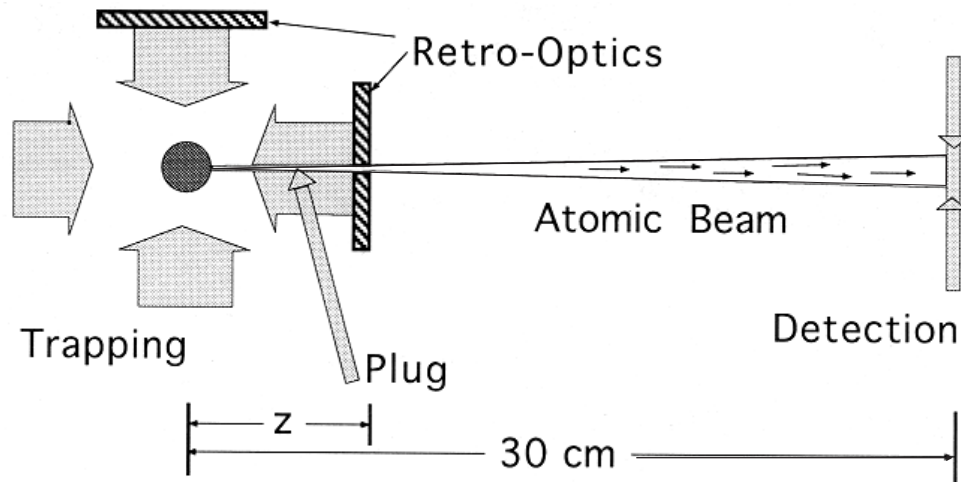


Figure 2.1: Schematic of the LVIS system. Large shaded arrows represent the 4 cm diameter trapping laser beams. A repump laser (not shown) illuminates the trapping volume up to the edge of the retro-optic, which has a small hole and is placed inside the vacuum chamber. This hole, a distance  $z$  from the trap center, creates an extraction column through the trap center and causes atoms to accelerate out of the VCMOT. A standing-wave light field 30 cm downstream forms the detection region. The plug is a thin beam of trapping laser light; when present, it prevents atoms from leaving the trap via the atomic beam.

the opposite direction to make six counter-propagating laser beams in a retro-reflecting configuration. The VCMOT beams are relatively large ( $\sim 4$  cm diameter) in order to maximize  $R$ . To produce the extraction column, a millimeter sized hole is drilled through the center of one of the retro-reflecting assemblies which consist of a quarter-wave plate and mirror<sup>1</sup>. The atomic beam is extracted from the trapping region through this hole. A pair of anti-Helmholtz coils generates the quadrupole magnetic field for the trap, with a gradient of  $\sim 5$  G/cm along the atomic beam direction. To position the trap center in the extraction column, the point of zero magnetic field is moved with a set of orthogonal magnetic shim coils. In normal operation, the plug beam is blocked by a mechanical shutter. When making measurements, the plug beam is unblocked so that the atoms are forced out of the extraction column and returned to the center of the trap. This capability of quickly turning the atomic beam on and off allows us to measure the longitudinal velocity distribution, and to run LVIS in a pulsed mode. With a CCD camera and a photo-diode, we monitor the fluorescence emitted when the atoms cross the detection region. This allows us to measure the flux, spatial distribution, and velocity distribution of the atomic beam.

<sup>1</sup> A hole was drilled in the quarter wave plate and then the back surface was coated with a reflecting layer of gold.

## 2.4 Results

### 2.4.1 Optimum Detuning

Given the trap parameters described above and in Fig. 2.1, we found that the trapping laser frequency which maximizes the LVIS beam flux is  $5 \Gamma$  detuned (where  $\Gamma$  is the natural line width) from the cycling transition, while the detuning that maximizes  $N$  in the normal VCMOT is  $3.2 \Gamma$ . This difference presumably occurs because the transverse light beams can heat and, if there are any imbalances, deflect the atomic beam as it exits the trap. At lower detunings, the scattering rates and hence these deleterious effects increase.

### 2.4.2 Longitudinal velocity

The longitudinal velocity distribution in the LVIS beam, as shown in Fig. 2.2, is measured by the time-of-flight method. Typically, we observe  $v \sim 15$  m/s, consistent with our simple model based on a calculation of the photon scattering rate from the forcing beam. In our model the acceleration begins when an atom enters the extraction column. As the atom is accelerated, the scattering rate slows due to Doppler shift and Zeeman shift. Scattering and acceleration cease when the atoms finally leave the region of repump light. Figure 2.3 shows the dependence of the longitudinal velocity on the intensity and frequency detuning of the forcing beam. Both plots indicate that the final velocity increases with the scattering rate in a manner consistent with our model. Note that the range of useful velocities is limited because the flux decreases rapidly when the intensity and detuning are far from those which optimize the trap capturing process.

A narrow longitudinal velocity distribution is usually desired in the applications of cold atomic beams. The velocity spread, about 2.7 m/s FWHM, is much larger than the Doppler cooling limit of 0.12 m/s. The velocity spreads due to a random distribution over magnetic sublevels and statistical fluctuations in the number of scattered photons were both estimated to be  $\sim 0.7$  m/s. We believe the dominant contribution to the longitudinal spread arises because the atoms enter the extraction column within the trap at different positions along the beam axis, and are therefore accelerated over different distances. A calculated velocity and spread match the experimentally observed values ( $v=14$  m/s, FWHM=2.7 m/s) if we assume that the acceleration distance covers the range 2.2 to 3.4 cm. This is reasonable since in this case  $z$  is 2.5 cm (see Fig. 2.1), and the atoms trapped in the VCMOT with the plug beam unblocked form a cloud  $\sim 1$  cm in diameter.

The fractional FWHM of the longitudinal velocity distribution depends on the forcing beam's polarization. Figure 2.4 shows that the fractional FWHM can be minimized by making the polarization significantly elliptical. For circularly polarized light, the Zeeman shift causes an atom to feel an acceleration which is much larger on the upstream side of the trap center than on the downstream side. This principle is essential to the operation of a MOT, but in a LVIS, atoms entering the extraction column on the upstream side experience a larger acceleration than those entering on the downstream side. However, an elliptically polarized forcing beam makes the accelerations more

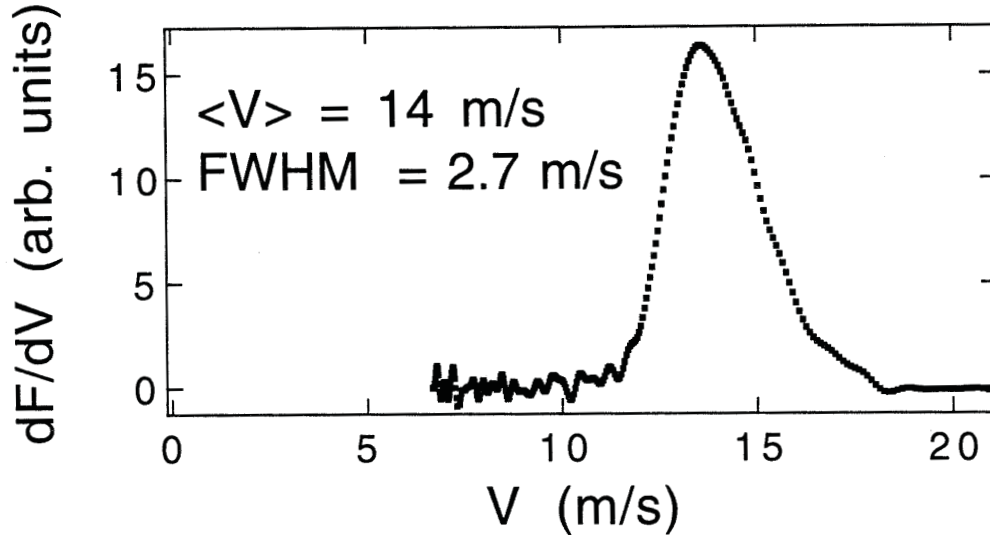


Figure 2.2: A typical longitudinal velocity distribution. In this case, the average velocity is 14 m/s and the FWHM is 2.7 m/s. This curve is made by first recording the shape of the time-of-flight (TOF) signal. The derivative of the TOF signal is then taken with respect to time, and time is converted into velocity using the known distance between the plug and the detection region. This yields the derivative of atom flux with respect to velocity, or the longitudinal velocity distribution.

nearly equal on the upstream and downstream sides. This results in a smaller final velocity spread. For angles  $<20^\circ$  and  $>70^\circ$ , the increased spatial spread in the trapped atom cloud outweighs this decreased variation in the acceleration.

### 2.4.3 Collimation

Many factors contribute at some level to the transverse collimation. Initially we expected transverse cooling and focusing within the extraction column to dominate. Instead, the measurements described below show that the transverse velocity distribution is primarily determined by a simple geometrical collimation mechanism. Although it is similar to the transverse velocity distribution of a conventional atomic beam collimated with physical apertures, the LVIS beam benefits because the apertured atoms are recycled. In LVIS, the collimation length ( $z$ ) extends from the point where atoms enter the extraction column to the mirror. The divergence angle of the atomic beam,  $\theta$ , is given by  $\theta \approx d/z$ , where  $d$  is the diameter of the extraction column. The spatial profile is consistent with the triangular profile expected from a geometrical collimation mechanism. When the extraction column was produced by placing the retro-optic with a hole at 2.9 cm from the trap center, the observed divergence angle (36 mrad) agrees well with  $d/z$  (40 mrad).

To further study this collimation mechanism, the retro-optic with a hole was re-

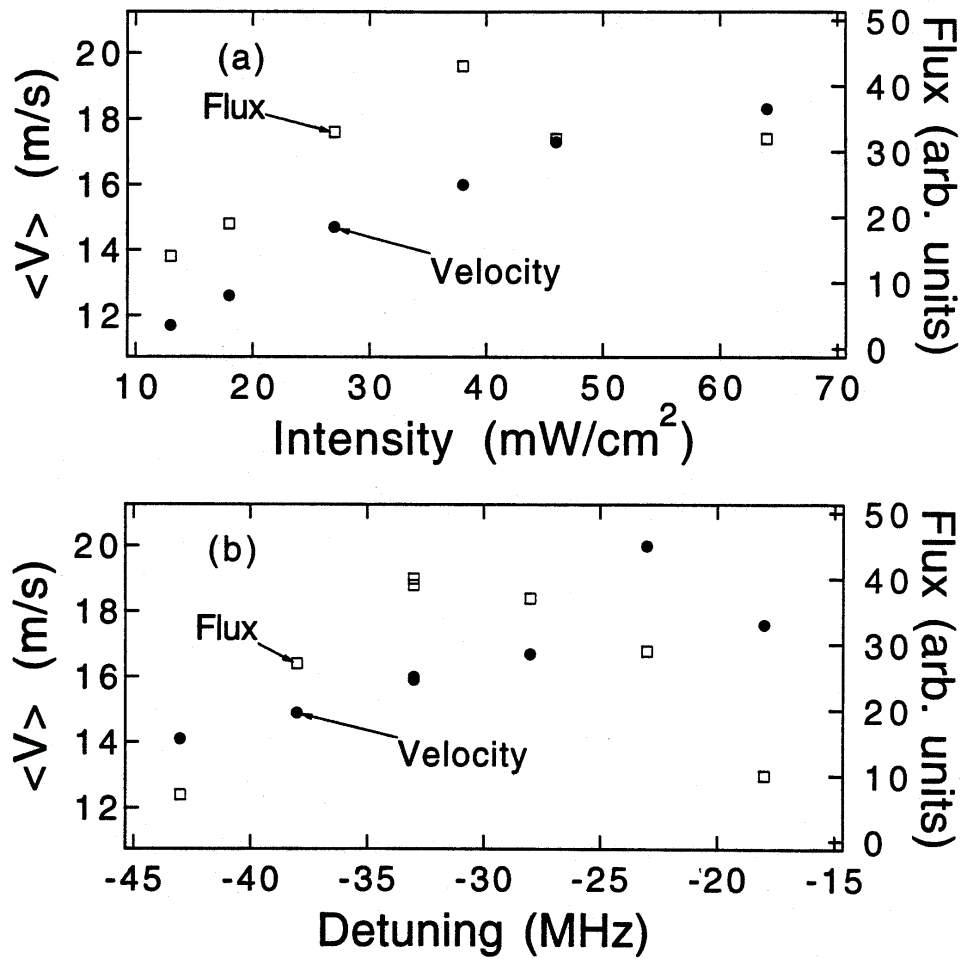


Figure 2.3: The average longitudinal velocity and flux as a function of (a) the forcing laser intensity (with detuning at 32 MHz) and (b) the detuning (with  $I=38 \text{ mW}/\text{cm}^2$ ). In both cases the final velocity increases with increasing scattering rate from the forcing beam, while the fractional spread remains nearly unchanged.

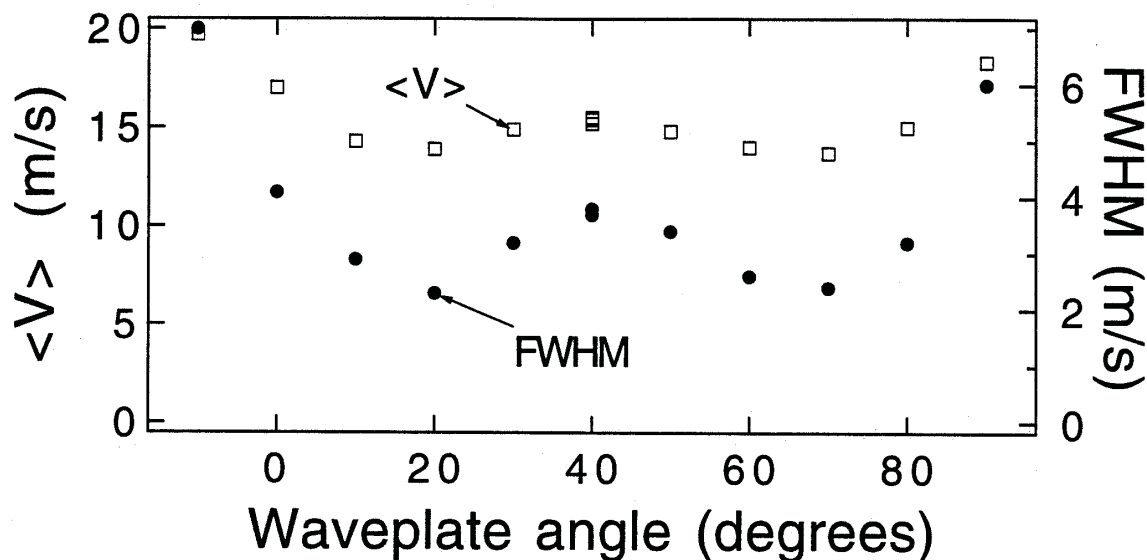


Figure 2.4: The average longitudinal velocity and spread as a function of the forcing beam polarization. The quarter-wave plate at  $45^\circ$  gives circularly polarized light. Below  $10^\circ$  and above  $80^\circ$  the flux falls rapidly because the trap capture rate decreases, but the flux varies by less than 30% between  $10^\circ$  and  $80^\circ$ . Also, the mean velocity has a much weaker dependence on polarization than the fractional spread.

placed by a standard retro-optic outside the vacuum chamber. We inserted a piece of glass with opaque spots of various sizes into the laser beam in front of the retro-optic to create the extraction column. To vary the collimation length, we varied the distance ( $z$ ) over which the repump laser illuminated the atomic beam. The divergence scaled with  $d/z$  over a wide range of conditions. Angle vs  $z$  is shown in Fig. 2.5. Note that while  $\theta$  scales as  $1/z$ , the measured values are consistently smaller than the opaque spot diameter divided by  $z$ . This is presumably due to diffraction of light into the extraction column which effectively makes  $d$  smaller than the diameter of the opaque spot.

The tightest collimation was achieved with our maximum collimation length (30 cm) and a 1.6 mm diameter opaque spot. We observed a divergence angle of 5 mrad, implying a transverse temperature of  $20 \mu\text{K}$ . This configuration requires careful alignment, and the atomic beam must be sent in a vertical direction to prevent gravity from pulling the atoms out of the extraction column.

To better understand the beam collimation, we replaced the conventional MOT field gradient with a quasi-two-dimensional MOT which had a magnetic field gradient of 7 G/cm in the transverse direction and  $<1$  G/cm in the longitudinal direction. We kept all other conditions the same. The atomic beam width changed from 1.1 mm to 0.65 mm when measured 3 cm above the trap center, but did not change when measured 30 cm above. Thus the quasi-two-dimensional configuration produced transverse focusing but not cooling.

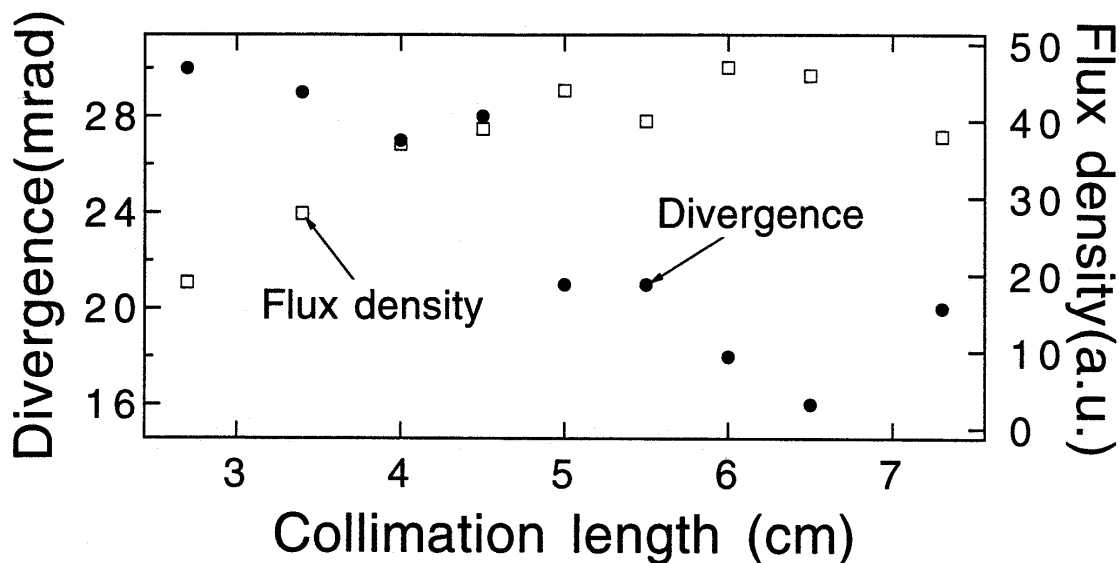


Figure 2.5: The measured divergence angle as a function of the collimation length  $z$ . The divergence angle decreases, consistent with a geometrical collimation mechanism. The flux density (in arbitrary units) increases until  $z \approx 6$  cm, indicating that the atoms are being captured back into the trap and recycled. For these measurements, the retro-optic was removed to the outside of the chamber, and the extraction column was generated by a 1.6 mm opaque spot such that the atoms were accelerated vertically.

#### 2.4.4 Flux

We measured the absolute atom flux in the LVIS beam and determined the atom transfer efficiency by comparing this flux with the capture rate of the VCMOT. The capture rate of the trap was determined from measurements of  $N$  and  $r_c$  with the plug beam in place. Our measurements indicated that essentially 100% of the atoms were transferred into the atomic beam for typical values of  $z$ . However, the fraction extracted through the hole in the retro-optic into a field-free region varied. The highest flux we achieved was  $5 \times 10^9/s$ , with an extraction efficiency of 30% ( $\theta=30$  mrad,  $d=0.7$  mm,  $z = 2.7$  cm) which was limited by light scattering around the hole edges. By making a cleaner hole through the retro-optic, ( $\theta= 36$  mrad,  $d=0.8$  mm,  $z=2.0$  cm) we increased the efficiency to 70%, but by that time, our deteriorating  $\text{Ar}^+$  laser tube allowed us to trap an order of magnitude fewer atoms. However, with this 70% efficiency and  $\sim 500$  mW of Ti:Sapphire laser power, we expect to achieve a beam flux  $>10^{10}/s$ . When operated at lower power the LVIS flux drops in proportion to the reduced capture rate for the MOT. However, the beam collimation and velocity remain nearly the same so LVIS would still produce a nice beam with low power diode lasers. Finally, we observed a much higher peak flux when the LVIS system was operated in a pulsed mode. In these geometries, the VCMOT empties in 50 ms, providing nearly the same time-averaged flux but ten times the peak flux and brightness.

The flux and flux density depend on the collimation angle and geometry of the LVIS setup in the manner predicted above. Although we achieved 70% extraction efficiency when  $\theta=36$  mrad, we only achieved a transfer efficiency of 20% when  $\theta=5$  mrad. Figure 2.5 shows the tradeoff between flux density and collimation of the atomic beam. Recycling causes the flux density (number  $\text{s}^{-1} \text{cm}^2$ ) at the detection region to increase while the divergence decreases. Total flux decreases beyond 4.5 cm because for a collimation this tight, the atomic beam transverse temperature becomes comparable to the temperature of atoms in the VCMOT. With tight collimations, an atom must make many more attempts to be successfully transferred into the atomic beam. This makes  $r_c/r_t$  larger, decreasing the flux as predicted.

## 2.5 Conclusion

We have created a slow, bright beam of cold atoms. We have observed the optimum detuning, beam collimation, and flux, and find them consistent with a geometrical collimation mechanism. A quasi two-dimensional quadrupole magnetic field did not improve the collimation. Finally, up to 70% of the atoms loaded into the MOT were continuously extracted into the beam, consistent with a recycling mechanism. The simplicity, brightness, and versatility of LVIS will make it useful in a wide range of applications.